Australian Journal of Crop Science AJCS
AJCS 6(2):238-247 (2012) ISSN:1835-2707

Simulation of salinity distribution in the overlap zone with double-point-source drip irrigation using HYDRUS-3D

Yuyang Shan[1,2], Quanjiu Wang[3,1*]

[1]State Key Laboratory of Soil Erosion and Dryland Farming on the Loess Plateau, Institute of Soil and Water Conservation, Chinese Academy of Sciences & Ministry of Water Resources, Yangling, Shaanxi 712100, PR China
[2]Graduate School of Chinese Academy of Sciences, Beijing 100049, PR China
[3]Institute of Water Resources, Xi'an University Technology, Xi'an; Shannxi 710048, PR China

***Corresponding author: wquanjiu@163.com**

Abstract

Salinity is a serious and chronic problem for agriculture in arid and semi-arid regions. Drip irrigation is widely used in such regions because it can decrease salinity in the soil. With drip irrigation, there is a region of confluence between each pair of emitters, termed the overlap zone, in which plants are grown. Hence, knowledge of the salinity distribution in the overlap zone is important to achieve high crop yields. The salinity distribution in and around the overlap zone was investigated empirically and in simulation (using HYDRUS-3D) for double-point-source drip irrigation with different irrigation volumes (8 L, 10 L, and 12 L) and emitter spacings (30 cm and 40 cm) in a sandy soil near Korla in Xinjiang Autonomous Region. The predictions from HYDRUS were found to be very close to the observed data in terms of the coefficient of correlation (R^2) and the root-mean-square error (RMSE). The R^2 varied from 0.69 to 0.92 and the RMSE from 0.003 to 0.008. Additional simulations with HYDRUS were used to evaluate the effects of various design parameters on the desalination zone. The relationship between irrigation volume and the size of the desalination zone was found to follow a power function (R^2 = 0.951), and that between emitter discharge and the size of the desalination zone was found to follow an exponential function (R^2 = 0.9995). A negative relationship was found between emitter spacing and the size of the desalination zone. For loam, the vertical extent of desalination was found to be about 1.3 times that of the horizontal. For loamy sand, the vertical extent of desalination far exceeded the horizontal extent, owing to its large hydraulic conductivity. We hope that these simulation results with HYDRUS-3D can provide a basis for designing suitable drip irrigation systems.

Keywords: salinity, drip irrigation, overlap zone, desalination zone, HYDRUS-3D.
Abbreviations: RWPT**-** random-walk particle-tracking; CDE**-** convection-dispersion equation; FVM**-** finite-volume method; MCM**-** Monte Carlo method; R^2**-** coefficient of correlation; RMSE**-** root-mean-square error.

Introduction

Soil salinity is frustrating the sustainable development of agriculture worldwide, particularly in arid and semi-arid regions. Wood et al. (2000) found that 20% of irrigated land suffers from salinization induced by the build-up of salts caused by poor irrigation. The design of a suitable and highly efficient irrigation system is vital for sustainable land utilization and crop production in such areas. Xinjiang in northwest China is typical of arid and semi-arid regions with freshwater scarcity. The salinity of most of the shallow groundwater sources in this region is greater than 2 dS m^{-1}. Hou et al. (2007) showed that about one-third (1.23×10^6 ha) of the total irrigated cropland in Xinjiang was affected by salinity, and Wang et al. (2008) suggested that salinity in the irrigated croplands of Xinjiang increased by 40% between 1983 and 2005. To alleviate this problem, various methods have been developed and drip irrigation is considered to be one of the most effective. Drip irrigation has been used worldwide for the past several decades. Its main advantages include: increased crop yields; reduced water application; decreased salinity; and deep percolation (Gao and Li, 2005; Zotarelli et al., 2009; Li et al., 2001; Ghosh et al., 2006; Cook et al., 2006; Li and Wang, 2009). Solute transport is a complicated problem. To better understanding of it, some analytical and numerical simulations have been developed to simulate solute transport in the soil. Most models of solute transport through soil consider steady advection (e.g., Dagan and Bresler, 1979; Broadbridge and White, 1988; Russo, 1993; Nachabe et al., 1995; Govindaraju et al., 1996). Marshall et al. (2000) concluded that steady advection models can adequately predict solute movement for small, temporal variations of the flow rate, but are inaccurate under highly transient flow (Beese and Wierenga, 1980; Islas and Illangasekare, 1992; Russo et al., 1994). The random-walk particle-tracking (RWPT) method has long been used to simulate conservative solute transport in porous media (Ahlstrom et al., 1977; Smith and Schwartz, 1980; Pickens and Grisak, 1981). Some studies have suggested that solute transport can be described by the classical convection-dispersion equation (CDE) in heterogeneous soils (Roth et al.,1991; Butters and Jury, 1989). Herrera et al. (2009) applied a meshless method to simulate solute transport in heterogeneous porous media. Huang and Zhou, (2010) used a coupling model to simulate solute transport in fractured rocks

Table 1. Goodness-of-fit of simulated to observed salinity under various scenarios.

Measurement	Emitter discharge (L h^{-1})	Emitter spacing (cm)	Irrigation volume (L)	R^2	RMSE*
Salinity	2.2	30	8	0.92	0.005
		30	10	0.90	0.004
		30	12	0.87	0.005
		30	10	0.92	0.003
		40	10	0.69	0.008

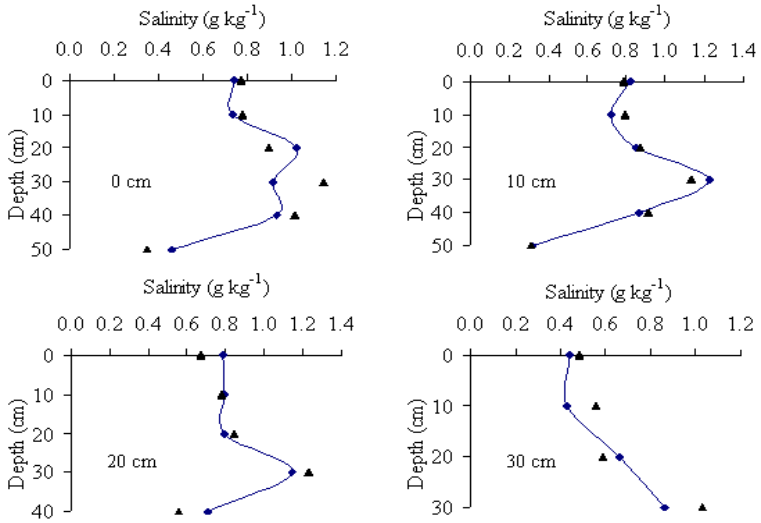

Fig 1. Measured and predicted salinity in the overlap zone for double-point-source drip irrigation with an irrigation volume of 10 L. The plots show the measured (solid line) and predicted (triangles) salinity along selected transects: 0, 10, 20, and 30 cm from the center of the overlap zone.

based on the finite-volume method (FVM). The results showed that the coupling model based on the FVM can be applied to the simulation of solute transport in a complicated fractured-rock system. Wang and Huang (2011) used the Monte Carlo method (MCM) (Cai, 2000) to evaluate the effect of permeability variations on solute transport in highly heterogeneous porous media. Currently the HYDRUS model (Šimůnek et al., 1999) is widely used for simulating solute transport with conventional and microdrip irrigation (Cote et al., 2003; Hassan et al., 2005; Gärdenäs et al., 2005). Abbasi et al. (2003) applied HYDRUS-2D to a simulation of water flow and solute transport below the furrow and found that HYDRUS-2D can simulate water and solute transport very well; as well as being an effective method for estimating soil hydraulic properties. Gärdenäs et al. (2006) applied HYDRUS-2D to a simulation of preferential water flow and pesticide transport in a tile-drained field and found that the model was suitable for studying pesticide leaching from undulating fields with large spatial variability in soil properties. Roberts et al. (2009) showed that HYDRUS-2D could predict salt accumulation with subsurface drip irrigation. The studies have shown the value of HYDRUS model as a tool for simulating solute dynamics with various irrigation systems. Under drip irrigation, confluence occurs between pairs of emitters and the area of confluence is termed the 'overlap zone', as well as plants (e.g., cotton) are always grown in the overlap zone between neighboring emitters in a field. In order to knowledge of salinity distribution in the overlap zone, Gu et al. (2009) was conducted some experiments with double-point-source drip irrigation, but only narrative phenomenon. Hence, the distribution of salinity in and around the overlap zone needs to be modeled accurately to ensure efficient crop production and soil conservation.

Although, simulation of salt transport around a single, isolated point-source emitter is a three-dimensional problem; it can be treated as two-dimensional problem in and around the overlap zone of neighboring emitters. Numerical modeling using HYDRUS (2D/3D) software (Šimůnek et al., 2006), which is widely used for simulating water, heat, and/or solute movement in two or three dimensions in variably-saturated porous media may be useful for this purpose. The objectives of this study were to: (1) investigate the performance of HYDRUS-3D for simulating the distribution of salinity under double-point-source drip irrigation, and (2) provide guidance for designing efficient drip-irrigation systems.

Results

Comparison of measured and simulated salinity

The measured and simulated salinity under drip irrigation in the overlap zone is shown in Figs. 1, 2, and 3 for irrigation volumes of 8, 10, and 12 L, respectively, and an emitter spacing of 40 cm. The measured and simulated salinity with emitter spacings of 30 and 40 cm are shown in Figs. 4 and 5, respectively, for an irrigation volume of 10 L. Each figure shows the measured and simulated salinity in the selected soil profile. From the plots shown in these figures, it is clear that the observed salinity distributions were very closely modeled by the simulations. To assess the accuracy of the model, the root-mean-square error (RMSE) and the coefficient of correlation (R^2) between the observed and simulated salinity were calculated. These goodness-of-fit statistics are reported in Table 1 for the three irrigation volume scenarios (8 L, 10 L, and 12 L) and the two emitter spacing scenarios (30 cm and 40 cm).

Table 2. Parameters used in HYDRUS-3D simulations.

Case	Soil type	Emitter spacing (cm)	Emitter discharge (L h^{-1})	Irrigation volume (L)	Water content (cm^3 cm^{-3})	Salinity (g kg^{-1})
I	Loam	30	1.8	8, 10, 12	0.15	10
II	Loam	40	1.8, 2.4, 3	12	0.15	10
III	Loam	30, 40	1.8	12	0.15	10
IV	Loam, Loamy sand	30	1.8	12	0.15	10

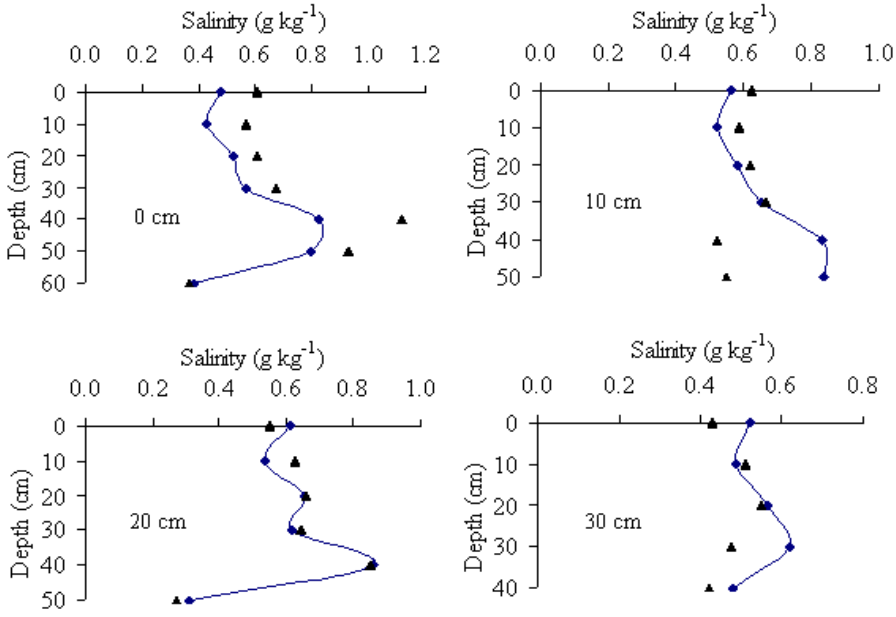

Fig 2. Measured and predicted salinity in the overlap zone with an irrigation volume of 10 L under double-point-source drip irrigation. The plots show the measured (solid line) and predicted (triangles) salinity along selected transects.

The RMSE ranged from 0.003 to 0.008 and the R^2 from 0.69 to 0.92. These results show that the model can accurately simulate spatial soil salinity distributions in the overlap zone under different conditions in the field. HYDRUS-3D has previously been shown to accurately simulate both temporal and spatial soil water content distributions, as well as the dimensions of the soil wetting pattern, at different emitter spacings with double-point-source drip irrigation on a clay loam soil (Wang et al., 2010). Kandelous et al. (2011) showed that the HYDRUS-3D could predict soil water content distributions between two emitters of a subsurface drip irrigation system. These results together show that the model could become a useful tool in the design, monitoring, and management of drip irrigation systems.

Discussion

The effect of various parameters-including irrigation volume, emitter spacing, emitter discharge rate, and soil texture on salinity distribution have been investigated previously (Khan, 1996; Wang et al., 2001; Lv et al., 2002; Wang et al., 2010), but few studies have considered the effect of these parameters on the shape of desalination zone, especially within the overlap zone. To investigate the effects of these parameters, additional simulations were conducted with HYDRUS-3D, using the information presented in Table 2.

Irrigation volume

The effect of irrigation volume on the shape of desalination zone (Table 2, Case I) is illustrated in Fig. 6, which shows that the larger the irrigation volume the larger the desalination zone. As the irrigation volume increased so did the vertical extent of the desalination zone, since the downward speed of the irrigation water was greater than its horizontal speed. In order to explore the relationship between the irrigation volume and the extent of desalination, the following equation was fit to the experimental data:

$$y = 10.488x^{1.2596} \qquad R^2 = 0.951$$

where y is the area of the desalination zone (cm^2) and x is the irrigation volume (L).

Emitter discharge rate

The effect of emitter discharge rate on the shape of the desalination zone (Table 2, Case II) is illustrated in Fig. 7. The figure shows that the area of the desalination zone increased as the rate of emitter discharge increased, since the water spread more rapidly horizontally than it did vertically, forming a larger pond on the surface. Note that the total volume of irrigation

Table 3. Hydraulic parameter values typical of particular soil textural classes (Carsel and Parrish, 1988)

Soil texture	θ_r ($cm^3\ cm^{-3}$)	θ_s ($cm^3\ cm^{-3}$)	α (cm^{-1})	n	K_s (cm min^{-1})	l	D_L (cm)	D_T (cm)
Loam	0.078	0.43	0.036	1.56	0.0173333	0.5	0.5	0.1
Loamy sand	0.057	0.41	0.124	2.28	0.243194	0.5	0.5	0.1

θ_r is the residual water content; θ_s the saturated water content; K_s is the saturated hydraulic conductivity; α is an empirical constant that is inversely related to the air-entry pressure; n is an empirical parameter related to the pore-size distribution; l is an empirical shape parameter; D_L is longitudinal dispersivity; and D_T is transverse dispersivity.

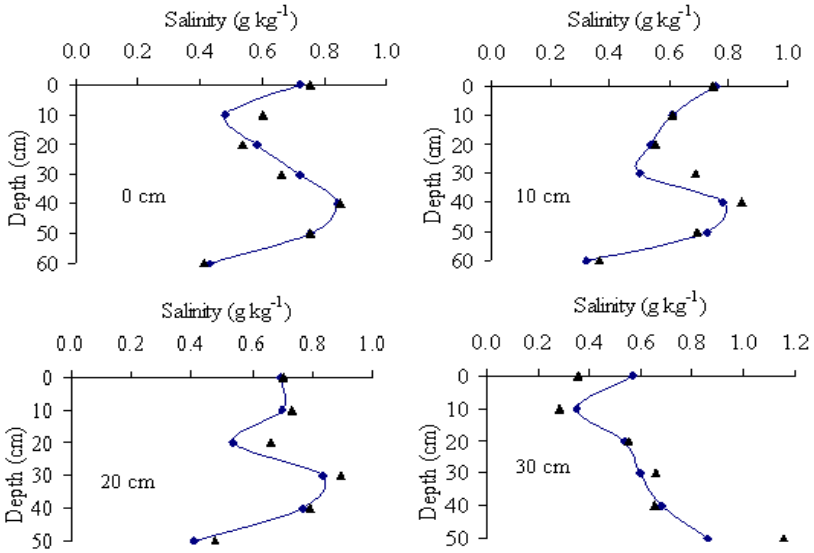

Fig 3. Measured and predicted salinity in the overlap zone with an irrigation volume of 12 L under double-point-source drip irrigation. The plots show the measured (solid line) and predicted (triangles) salinity along selected transects

water was constant in these three simulations. At depths of 0–20 cm, as the emitter discharge rate increased, the salinity decreased; at depths of 20–25 cm, the inverse relationship held. In order to explore the relationship between emitter discharge rate and extent of desalination, the following equation was fit to the experimental data:

$$y = 269.27\,In(x) - 159.02\,, \qquad R^2 = 0.9995$$

where y is the area of the desalination zone (cm^2) and x is the emitter discharge rate (L h^{-1}).

Emitter spacing

We simulated the salinity distribution with HYDRUS-3D for emitter spacings of 30 and 40 cm (Table 2, Case III). The salinity profile (illustrated in Fig. 8) shows that there was a desalination zone of 248.9 cm^2 when the emitter spacing was 30 cm but an accumulation zone when the emitter spacing was 40 cm. There was a negative correlation between emitter spacing and irrigation volume. This is because with a wider emitter spacing, the wetting fronts must travel further in order to intersect, yet the rate of advance of the wetting fronts slows over time.

Soil texture

The effect of soil texture on the shape of the desalination zone (Table 2, Case IV) was investigated using the soil hydraulic parameter values given in Table 3, which are typical for these soil texture classes (Carsel and Parrish, 1988). For the two soil types considered, the bulk density was 1.5 g cm^{-3}. The predicted desalination zone and distribution of salinity in the overlap zone are illustrated in Fig. 9. The figure shows that the desalination zone was smaller for loamy sand than for loam in the horizontal direction and larger in the vertical direction. For the soil textures considered, the desalination downwards, due to gravity, was greater than it was horizontally. The loamy sand had a larger hydraulic conductivity, resulting in greater desalination downwards and a non-uniform distribution, whereas the distribution was fairly uniform for loam. For loam, the extent of desalination downwards was about 1.3 times that horizontally, but the ratio was far higher for loamy sand. In order to improve the desalination in the horizontal plane for loamy sand, we would need to apply higher emitter discharge rates and/or smaller emitter spacings.

Materials and Methods

Field experiments were conducted in 2010 at the irrigation management station for BaZhou prefecture in Xinjiang, near the capital, Korla (41° 35′ N, 86° 10′ E; altitude 903 m). The region is classified as a warm-temperate arid zone with continental climate (Wei et al., 2009). The mean annual precipitation is approximately 53.3–62.7 mm, most of which occurs between June and August; the mean annual evaporation from free water surfaces varies from 2273 to 2788 mm; the mean annual relative humidity varies from 45% to 47%; the mean annual temperature is 10.5°C; the long-term mean maximum air temperature is 43.6°C in July; the long-term mean minimum air temperature is -9.4°C in January; the annual total sunshine is 3036 h; and the mean number of frost-free

Table 4. Soil characteristics of the experiment field.

Depth (cm)	Bulk denstiy (g cm^{-3})	Clay (%)	Silt (%)	Sand (%)
10	1.53	5.3	22.7	72
20	1.51	6.6	26.9	66.5
30	1.48	5.9	24.8	69.3
40	1.49	5.9	24.5	69.6
50	1.45	5.6	23.3	71.1
60	1.59	2.4	8.8	88.8
Average	1.51	5.3	21.8	72.9

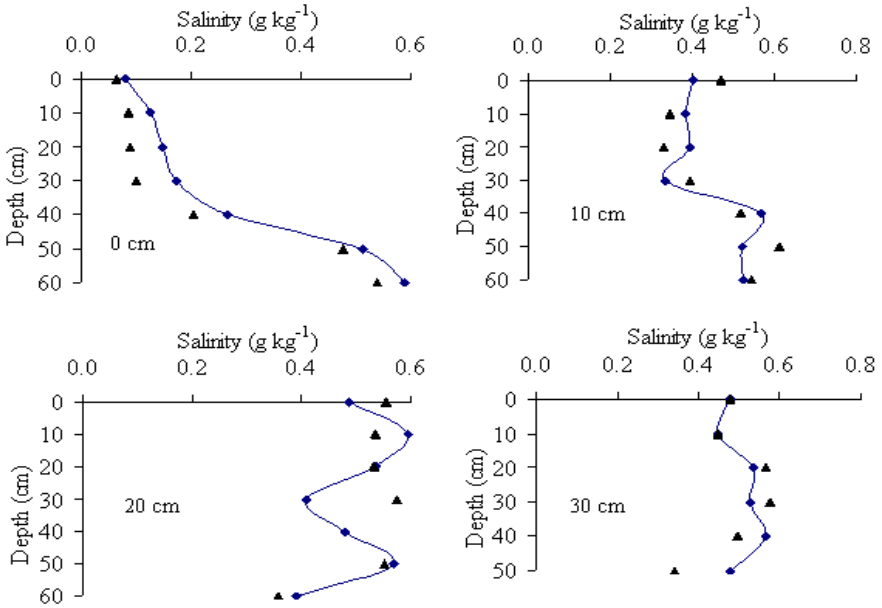

Fig 4. Measured and predicted salinity in the overlap zone with an emitter spacing of 30 cm under double-point-source drip irrigation. The plots show the measured (solid line) and predicted (triangles) salinity along selected transects.

days per year is 188. Measured values of the physical properties of the soil are given in Table 4, including the soil bulk density (from Blake and Hartge, 1986) and percentage of sand, silt, and clay (from Gee and Or, 2002), at the depths 0–10, 10–20, 20–30, 30–40, 40–50, and 50–60 cm. The soil at the experimental site is classified as sandy.

Field experiments

Two sets of experiments were performed on double-point-source drip irrigation in an uncultivated field. The two sets of experiments concerned only salinity distribution in the overlap zone.

Experiment 1: Different irrigation volume

The first set of experiments was conducted on 19 September 2010. The emitter discharge rate (water application per hour) was 2.2 L h^{-1} and the emitter spacing was 40 cm (Fig. 10). The irrigation volume was 8 L, 10 L, or 12 L. The average initial volumetric water content and salinity of the soil were 0.043 cm^3 cm^{-3} and 0.42 g kg^{-1}, respectively.

Experiment 2: Different emitter spacing

The second set of experiments was conducted on 21 September 2010. The emitter discharge was 2.2 L h^{-1}. The emitter spacing was 30 cm or 40 cm (Fig. 11). In both cases the irrigation volume was 10 L. The average initial volumetric water content and salinity of the soil were 0.038 cm^3 cm^{-3} and 0.32 g kg^{-1}, respectively.

Irrigation and collected samples

The mineral content of the irrigation water was 0.8 g L^{-1} and was considered to be freshwater (Ma et al., 2001). Mariotte bottles (10 cm inner diameter, 50 cm height) were used for water application. During the experiments, the water level of the Mariotte bottles was measured to calculate the cumulative infiltration. Each experiment had two Mariotte bottles and two laterals. Each lateral had a control valve to regulate emitter discharge. The timing of water application was measured with a stopwatch. Following irrigation, soil samples were taken in the plane bisecting the overlap zone, equidistant from the two emitters. Samples were taken 0, 10, 20, and 30 cm from the center of the overlap zone at depths of 0, 10, 20, 30, 40, 50, and 60 cm. The samples were weighed as collected then dried at 105°C for 24 h, and re-weighed to determine the water content (Gardner, 1986). Volumetric water content was determined by multiplying gravimetric water content by an average bulk density of 1.51 g cm^{-3}. Soil salinity (S; g kg^{-1}) was determined by measuring the electrical conductivity (EC; mS cm^{-1}) of a

Table 5. Estimated soil hydraulic parameters.

θr ($cm^3\ cm^{-3}$)	θs ($cm^3\ cm^{-3}$)	α (cm^{-1})	n	Ks ($cm\ min^{-1}$)	l	D_L (cm)	D_T (cm)
0	0.37	0.1058	1.993	2.447	0.5	2.97	0.01

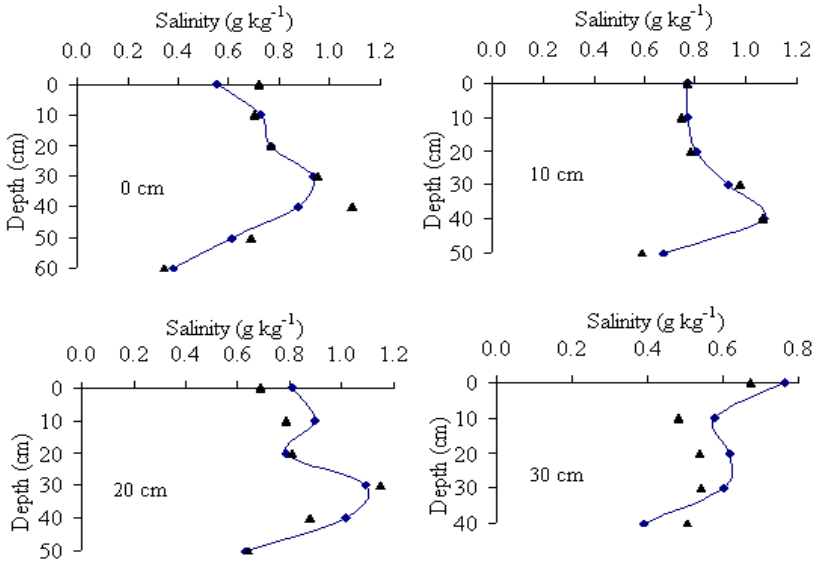

Fig 5. Measured and predicted salinity in the overlap zone with an emitter spacing of 40 cm under double-point-source drip irrigation. The plots show the measured (solid line) and predicted (triangles) salinity along selected transects.

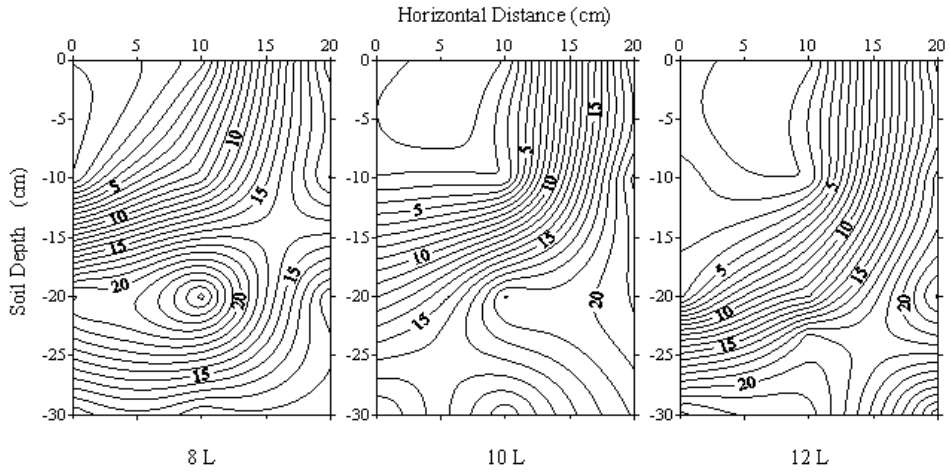

Fig 6. Predicted desalination zone and salinity distribution in the overlap zone for different irrigation volumes with double-point-source drip irrigation.

water:soil (5:1) mixture with a DDS-307A conductivity meter (Shanghai Precision & Scientific Instrument Inc., Shanghai, China) and the relationship: S = 4.352×EC.

Salt transport simulation

Salt transport in soil is controlled by both infiltration and diffusion. It can be described by the CDE (Bear, 1972). In the HYDRUS-3D model, CDE equation is solved numerically using Galerkin-type linear finite element schemes. To solve the CDE, we need to know the values of solute transport parameters, including the longitudinal dispersion coefficient (D_L) and the transverse dispersion coefficient (D_T). Some others hydraulic parameters also need to be known, including θ_s, θ_r, K_s, α, n, l. We estimated the hydraulic parameters using the inverse solution included in the HYDRUS-3D package. The estimated parameters are given in Table 5. For the simulations, two transport domains were designed: one was a rectangular parallelepiped (50 cm long, 30 cm wide, and 60 cm deep; discretized with 9540 nodes) as shown in Fig. 12 and another was rectangular parallelepiped (50 cm long, 40 cm wide, and 60 cm deep; discretized with 13,040 nodes) in Fig. 13.

Initial and boundary conditions

For the experiments modeled here, we chose the initial solute

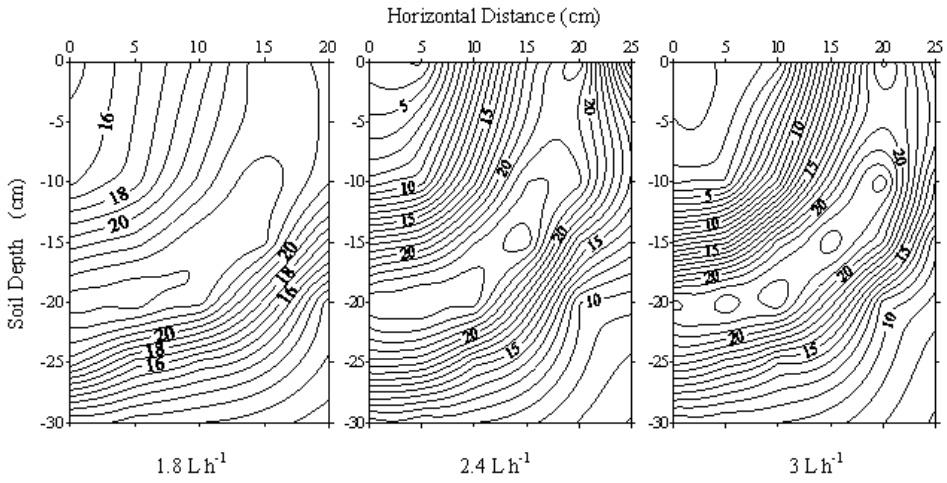

Fig 7. Predicted desalination zone and salinity distribution in the overlap zone for different emitter discharge rates with double-point-source drip irrigation.

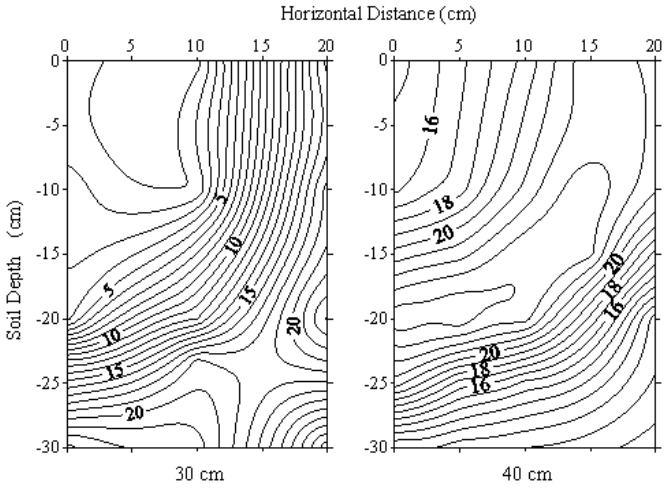

Fig 8. Predicted desalination zone and salinity distribution in the overlap zone for different emitter spacings with double-point-source drip irrigation.

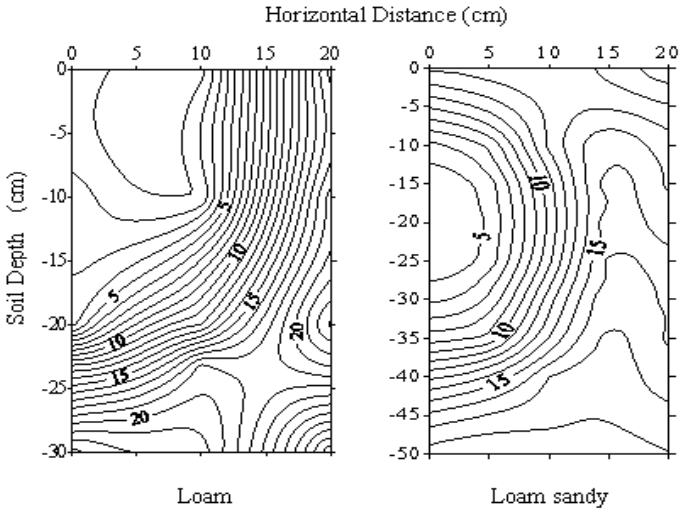

Fig 9. Predicted desalination zone and salinity distribution in the overlap zone for different soil textures with double-point-source drip irrigation.

concentration within the flow domain throughout the soil profile. A third-type (Cauchy type) boundary condition is used to prescribe the concentration flux. A free drainage boundary

condition was applied along the lower boundary. Information concerning implementation of these boundary conditions can be found in the HYDRUS (2D/3D) user manual (Šimůnek et al. 2006). When each irrigation event is finished, the upper and lower boundaries become zero-flux boundaries. Both during and after irrigation, zero-flux boundary conditions were used for all three dimensions.

Statistical analysis

The coefficient of correlation (R^2) and the root-mean-square error (RMSE) between simulated and measured values are commonly used to evaluate model performance (Siyal and Skaggs, 2009; Kandelous and Šimůnek, 2010; Kandelous et al., 2011). These statistics are described in Willmott (1982). We employed both methods to provide a quantitative comparison of the goodness-of-fit of the simulated salt content to the measured one.

Conclusions

In this study, we used the HYDRUS-3D model to simulate the salinity distribution in and around the overlap zone for double-point-source drip irrigation under different conditions in the field. The observed and simulated values were very close, demonstrating that the HYDRUS-3D model can accurately

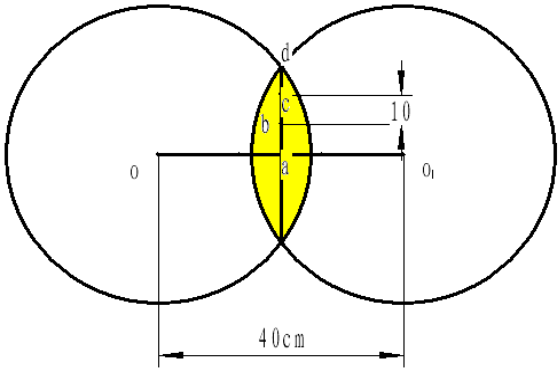

Fig 10. Layout of experiment 1 in the field; o, o_1: emitters; a, b, c, d: sampling locations; yellow: overlap zone.

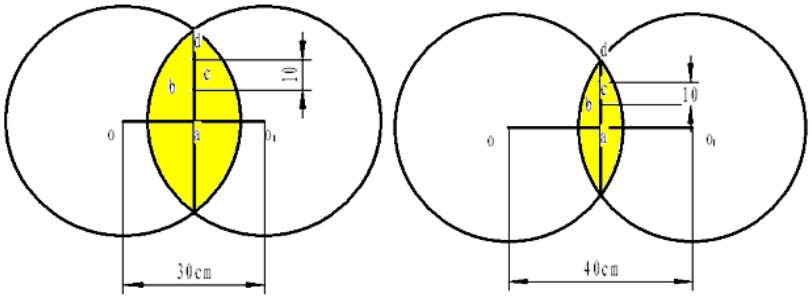

Fig 11. Layout of experiment 1 in the field; o, o_1: emitters; a, b, c, d: sampling locations; yellow: overlap zone.

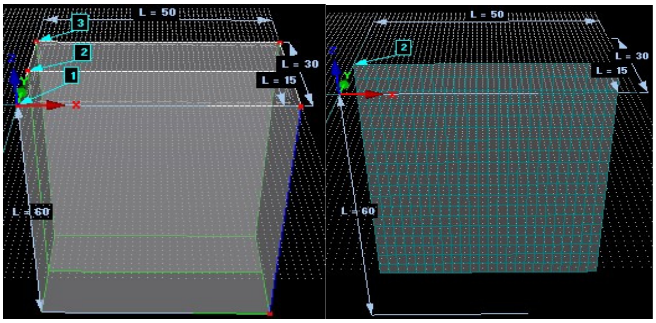

Fig 12. Left: typical geometry and finite-element mesh used in the HYDRUS-3D simulations; 1, 3: emitters; 2: center of the overlap zone. Right: the plane bisecting the overlap zone

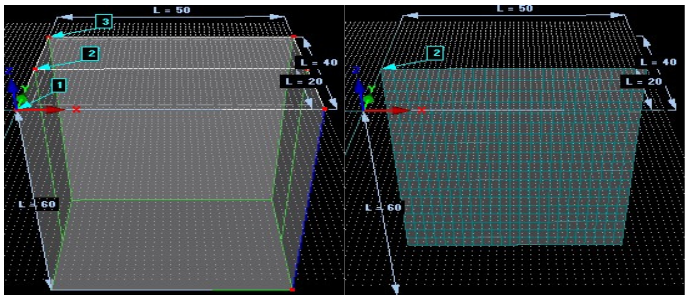

Fig 13. Left: typical geometry and finite-element mesh used in the HYDRUS-3D simulations; 1, 3: emitters; 2: center of the overlap zone. Right: the plane bisecting the overlap zone.

simulate salt transport under these conditions. We also evaluated the effects of a number of factors on the shape of the desalination zone, including irrigation volume, discharge rate, emitter spacing, and soil type. The simulation results showed that the area of the desalination zone was: (1) positively correlated with irrigation volume, following a power function; (2) positively correlated with discharge rate, following an exponential function; and (3) negatively correlated with emitter spacing. The simulation results also showed that, for the coarser soil type, the extent of desalination was far greater vertically than it was horizontally. We hope that these results can provide a robust framework for designing drip irrigation systems. In the future, we intend to employ HYDRUS-3D to explore the effect of other factors on the salinity distribution and desalination zone.

Acknowledgements

The authors would like to thank the National Key Technology R&D Program (2007BAD38B01) and the National High Technology Research and Development Program of China (2006AA100207) as well as the National Natural Science Foundation of China (50879067) for funding this work. Special and sincere thanks go to the two anonymous reviewers for their useful comments and suggestions.

References

Abbasi F, Feyen J, van Genuchten MT (2004) Two-dimensional simulation of water flow and solute transport below furrows: model calibration and validation. J Hydrol 290: 63-79

Ahlstrom S, Foote H, Arnett R, Cole C, Serne R (1977) Multicomponent mass transport model: theory and numerical implementation (discrete–parcel–random–walk version) Tech. rep., BNWL-2127, Battelle Pacific Northwest Labs., Richland, Wash. (USA)

Bear J (1972) Dynamics of fluids in porous media. Elsevier, New York

Beese F, Wierenga PJ (1980) Solute transport through soil with adsorption and root water uptake computed with a transient and a constant-flux model. Soil Sci 129: 245-252

Blake GR, Hartge KH (1986) Particle density. In: Klute A (Ed) Methods of soil analysis. Soil Science Society of America: Madison, WI, 377-382

Brandt A, Bresler E, Diner N, Ben-Asher I, Hiller J, Goldberg D (1971) Infiltration from a trickle source I. Mathematical model. Soil Sci Soc Am J 35: 675-682

Broadbridge P, White I (1988) Constant rate rainfall infiltration: a versatile nonlinear model: 1. Analytical solution. Water Resour Res 24: 145-154

Butters GL, Jury WA (1989) Field-scale transport of bromide in an unsaturated soil: 2. Dispersion modeling. Water Resour Res 25(7): 1583-1589

Carsel RF, Parrish RS (1988) Developing joint probability distributions of soil water retention characteristics. Water Resour Res 24: 755-769

Cook HF, Valdes GSB, Lee HC (2006) Mulch effects on rainfall interception, soil physical characteristics and temperature under *Zea mays* L. Soil Till Res 91: 227-235

Dagan G, Bresler E (1979) Solute dispersion in unsaturated heterogeneous soil at field scale: I. Theory. Soil Sci Soc Am J 43: 461-467

Gardner WH (1986) Water content. In: Klute A (Ed) Methods of soil analysis. Soil Science Society of America: Madison, WI, 493-544

Gärdenäs AI, Šimůnek J, Jarvis N, van Genuchten MT (2006) Two-dimensional modelling of preferential water flow and pesticide transport from a tile-drained field. J Hydrol 329: 647-660

Gee GW, Or D (2002) Particle-size analysis. In: Dane JH, Topp GC (Ed) Methods of Soil Analysis, Part 4-Physical Methods. Soil Science Society of America: Madison, WI, 255-293

Ghosh PK, Dayal D, Bandyopadhyay KK, Mohanty M (2006) Evaluation of straw and polythene mulch for enhancing productivity of irrigated summer ground nut. Field Crops Res 99: 76-86

Govindaraju RS, Kavvas ML, Jones SE, Rolston DE (1996) Use of Green–Ampt model for analyzing one-dimensional convective transport in unsaturated soils. J Hydrol 178: 337-385

Gu XB, Hu DT, Cao W, Liu JR, Qiao LP (2009) Laboratory experimental study on soil-water movement with double point source of drip irrigation. Yellow River 31: 88-91 (in Chinese)

Herrera PA, Massabó M, Beckie RD (2009) A meshless method to simulate solute transport in heterogeneous porous media. Adv Water Res 32: 413-429

Hou ZA, Li PF, Gong J, Wang YN (2007) Effect of different soil salinity levels and application rates of nitrogen on the growth of cotton under drip irrigation. Chinese J Soil Sci 38: 681-686 (in Chinese with an English abstract)

Huang Y, Zhou ZF (2010) Simulation of solute transport using a coupling model based on the finite volume method in fractured rocks. J Hydrodyn Ser B 22(1): 129-136

Islas AL, Illangasekare TH (1992) Solute transport under a constant infiltration rate: 1. Analytical solutions. In: Morel-Seytoux H (Ed.), Abstracts of Annual American Geophysical Union, Hydrology Days. American Geophysical Union, vol. 57. Selby Lane, Atherton, CA 94027

Kandelous MM, Šimůnek J (2010) Numerical simulations of water movement in a subsurface drip irrigation system under field and laboratory conditions using HYDRUS-2D. Agric Water Manage 97: 1070-1076

Kandelous MM, Šimůnek J, van Genuchten MT, Malek K (2011) Soil water content distributions between two emitters of a subsurface drip irrigation system. Soil Sci Soc Am J 75: 488-497

Khan (1996) Field evaluation of water and solute distribution of point source. J Irrig Drain Eng 122: 221-227

Li XD, Wang J (2009) Changes of soil salinity and determination of optimal salt washing mode in the condition of drip irrigation under plastic film of cotton in Xinjiang. Bull Soil Water Conserv 29(1): 115-118 (in Chinese with an English abstract)

Li Y, Wang WY, Wang QJ (2001) A breakthrough thought for water saving and salinity control in arid and semi-arid area under-film trickle irrigation. J Irrig Drain 20(2): 42-46 (in Chinese with an English abstract)

Lockington D, Parlange JY, Surin A (1984) Optimal prediction of saturation and wetting fronts during trickle irrigation. Soil Sci Soc Am J 48: 488-494

Lv DQ, Wang QJ, Wang WY, Shao MA (2002) Salt distribution and effect factors in under-film drip irrigation. J Irrig Drain 20: 28-31 (in Chinese with an English abstract)

Ma TL, Yuan BH, Mei JD (2001) Feasibility analysis on irrigation return flow reuse system in Hetao irrigation district in Inner Mongolia. J Irrig Drain 20(2): 69-72 (in Chinese with an English abstract)

Marshall JD, Shimada BW, Jaffe PR (2000) Effect of temporal variability in infiltration on contaminant transport in the unsaturated zone. J Contam Hydrol 46: 151-161

Nachabe MH, Islas AL, Illangasekare TH (1995) Analytical solutions for water-flow and solute transport in the unsaturated zone. Ground Water 33: 304-310

Pickens J, Grisak G (1981) Scale-dependent dispersion in stratified granular aquifer. Water Resour Res 17(4):1191-1211

Roth K, Jury WA, Fluhler H, Attinger W (1991) Transport of chloride through an unsaturated field soil. Water Resour Res 27(10): 2533-2541

Russo D (1993) Stochastic modeling of macrodispersion for solute transport in a heterogeneous unsaturated porous formation. Water Resour Res 29: 383-397

Russo D, Zaidel J, Laufer A (1994) Stochastic analysis of solute transport in partially saturated heterogeneous soil**:** 2. Prediction of solute spreading and breakthrough. Water Resour Res 30: 781-790

Šimůnek J, Šejan M, van Genuchten MT (1999) The HYDRUS-2D software package for simulating two-dimensional movement of water, heat and multiple solutes in variably saturated media, version 2.0. Rep. IGCWMC-TPS-53, Int. Ground Water Model. Cent., Colo. Sch. of Mines, Golden, CO, p. 251

Šimůnek J, Šejan M, van Genuchten MT (2006). The HYDRUS soft ware package for simulating two-and three-dimensional movement of water, heat, and multiple solutes in variably-saturated media. Technical Manual, Version 1.0. PC Progress, Prague, Czech Republic

Siyal AA, Skaggs TH (2009) Measured and simulated soil wetting patterns under porous clay pipe sub-surface irrigation. Agric Water Manage 96: 893-904

Smith L, Schwartz FW (1980) Mass transport.1. A stochastic analysis of macroscopic dispersion. Water Resour Res 16(2): 303-313

Wang CX, Wang QJ, Liu JJ, Zhang M, Zhuang L, Pan HB (2010) Trial studies on characteristics of soil water and salt distribution in brackish water drip irrigation. Agric Res Arid Areas 28(6): 30-35 (in Chinese with an English abstract)

Wang KL, Huang GH (2011) Effect of permeability variations on solute transport in highly heterogeneous porous media. Adv Water Res 34(6): 671-683

Wang QJ, Wang WY, Wang ZR, Zhang JF, Li Y (2001) Determination of technique parameters for saline-alkali soil through drip irrigation under film. Trans Chin Soc agri Eng 17(2): 47-50 (in Chinese with an English abstract)

Wang WJ, Niu WQ, SunYQ, Wu P (2010) Simulation study on the effects of dripper spacing on soil water infiltration conditions under surface drip irrigation with two point-source emitter. J Northwest Agric For Univ (Nat. Sci. Ed.) 38(4): 219-225 (in Chinese with an English abstract)

Wang YG, Xiao DN, Li Y, Li XY (2008) Soil salinity evolution and its relationship with dynamics of groundwater in the oasis of inland river basins: case study from the Fubei region of Xinjiang Province, China. Environ Monit Assess 140: 291-302

Wei GH, Dong XG, Yang PN, Yang XX, Yao PL (2009) Study on soil salt movement in drip irrigation of cotton under the plastic mulch. Res Soil Water Conserv 16(6): 162-166 (in Chinese with an English abstract)

Willmott CJ (1982) Some comments on the evaluation of model performance. Bull Am Meteorol Soc 63 (11): 1309-1313

Wooding RA (1968) Steady infiltration from a shallow circular pond. Water Resour Res 4 (6): 1259-1273

Wood S, Sebastian K, Scherr SJ (2000) Soil resource condition. In: Wood et al. (Eds.), Pilot Analysis of Global Ecosystems. IFPRI and World Resources Institute, Washington, DC

Zotarelli L, Scolberg JM, Dukes MD, Munoz-Carpena R (2009) Tomato yield, biomass accumulation, root distribution and irrigation water use efficiency on a sandy soil, as affected by nitrogen rate and irrigation scheduling. Agric Water Manage 96: 23-34